Morphological analysis of the urethral muscle of the male pig with relevance to urinary continence and micturition

doi: 10.1111/joa.12415

Morphological analysis of the urethral muscle of the male pig with relevance to urinary continence and micturition

Luisa Ragionieri, Francesca Ravanetti, Ferdinando Gazza, Maddalena Botti, Ana Ivanovska and Antonio Cacchioli

Department of Veterinary Sciences, University of Parma, Parma, Italy

Abstract

To investigate whether the pig could be considered a suitable model to study lower urinary tract function and dysfunction, the pelvic urethra of 24 slaughtered male pigs were collected, and the associated muscles were macroscopically, histologically and histochemically analyzed. In cross-sections of the urethra, a muscular complex composed of an inner layer of smooth muscle and an outer layer of striated muscle that are not separated by fascial planes was observed. A tunica muscularis, composed of differently oriented smooth muscle bundles, is only evident in the proximal part of the pelvic urethra while, in the remaining part, it contributes to form the prostatic fibromuscular stroma. The striated urethral muscle surrounds the pelvic urethra in a horseshoe-like configuration with a dorsal longitudinal raphe, extending from the bladder neck to the central tendon of perineum. Proximally to the bladder, it is constituted of slow-twitch and fast-twitch myofibers of very small diameter, and embedded in an abundant collagen and elastic fiber net. Moving caudally it is gradually encircled and then completely substituted by larger and compact myofibers, principally presenting circular orientation and fast-twitch histochemical characteristics. So, like in humans, the cranial tract of the muscular system surrounding the pelvic urethra is principally composed of smooth musculature. The striated component cranially may have a role in blocking retrograde ejaculation, while the middle and caudal tracts may facilitate urine and semen flow, and seem especially concerned with the rapid and forceful urethral closure during active continence. Some differences in the morphology and structure between pigs and humans seem due to the different morphology of the 'secondary' sexual organs that develop from the urethral wall and to the different effect of gravity on the mechanics of the urinary system in quadruped and bipedal mammals.

Key words: histochemistry; histology; male pig; transmission electron microscopy; urethral muscle.

Introduction

Constriction of the urethra prevents urine leakage but, despite a century of investigations, there is some controversy about which structures provide continence. At least in humans, one of these structures seems to be the urethral muscle (UM; Strasser et al. 2000), a muscle composed of specialized striated fibers, probably developing for transdifferentiation of smooth to striated muscle (Borirakchanyavat et al. 1997). It lies outside, but intimately associated with, the urethral tunica muscularis and extends from the bladder neck to the central tendon of perineum. It is more voluminous, developed and better defined in males than in females, generally thickest on the ventral side of the urethra, and thin or absent dorsally.

Most studies on the morphology and function of the UM, essential for solving problems of urinary incontinence seriously compromising the quality of life of men and women of any age, have been performed on biopsies or cadavers. However, research in the field of urinary continence requires an animal model with an UM similar to that of humans regarding size, function and histopathological anomalies associated with sphincter insufficiency. In males, the association of the UM with 'secondary' sexual organs varies depending on the species and age. Modifications in the orientation, morphology, size, type and number of the myofibers occur at puberty, when the prostate, developed from the urethra, further grows into the overlying striated

Correspondence
Ferdinando Gazza, Department of Veterinary Sciences, University of Parma, Via del Taglio 10, 43126 Parma, Italy. T: +39 521 032647; E: ferdinando.gazza@unipr.it

Accepted for publication *13 October 2015*

muscle, and continues in the adult as a result of the infiltration of connective tissue and vascular plexuses, followed by degenerative changes in the prostate (Oelrich, 1980).

Histochemical, biochemical and ultrastructural studies documented that in humans (Elbadawi, 1996; Creed & Van der Werf, 2001), guinea pig (Whitmore et al. 1984), rabbit (Tokunaka et al. 1986), cat (Elbadawi, 1985), dog, sheep (Chen & Creed, 2004) and female pig (Zini et al. 2006), the action of the UM is mediated by both aerobic type I fibers (Gosling et al. 1981), adapted to sustain long periods of contraction, and type II myofibers, which develop fast and strong contraction but are rapidly fatigued. Most studies using animal models, however, revealed significant differences from the human anatomy (Neuhaus et al. 2001; Stolzenburg et al. 2002) in the percentage and distribution of these fiber types within the UM, so further investigations are necessary. To the authors' knowledge, research on the UM of the swine species was previously done only in the female (Dass et al. 2001; Zini et al. 2006). As information on the male pig is scanty, a pilot study was performed to evaluate if it could be considered a good biological model for research in the field of urinary continence, analyzing its morphostructural features by means of macroscopic observations and histological and histochemical techniques, and comparing the current data with what is reported in literature on humans.

Materials and methods

Bladders and pelvic urethras were obtained at a local slaughterhouse from 24 adult (8–9 months old) male pigs, weighing about 180 kg, immediately after death. The pelvic urethras of six pigs were longitudinally sectioned to measure variations in the UM thickness, the other 18 samples were transversally sectioned into seven parts of about 2 cm in length, that were labeled with letters from A to G in the cranio-caudal direction. The first two cranial (A and B), the intermediate (D) and the most caudal part (G) were then considered for microscopic analysis.

Histology, histochemistry and histomorphometry

After routine preparation of paraffin-embedded tissues for histology, for each part of the pelvic urethra from six pigs four cross-sections (9 μm) were chosen at approximately 5 mm intervals, which were alternatively stained with Masson trichrome staining, to highlight collagenous connective tissue, and Orcein method, elective for elastic fibers. The specimens collected from the other six animals were cross-sectioned, frozen in isopentane, cooled in liquid nitrogen and subsequently cut with a cryostat (Microm HM 505 E; Microm International, Germany). Fiber types distribution patterns were studied on serial sections stained for myofibrillar ATPase after preincubation at different pH values (pH 4.2, 4.6 and 10.6) using the method described by Brooke and Kaiser (1970) with modifications. In the present investigation the various subtypes of type II fibers were did not distinguished between.

The histological sections were analyzed with a microscope Nikon Eclipse 90i (Nikon, Tokyo, Japan) equipped with a digital camera (Nikon model 5M) and an image analysis software (NIS – Elements AR 3.1; Nikon).

Histomorphometric assessment was performed on Masson trichrome-stained sections, within three square regions of interest (ROIs) of 500 μm side, counting the number of whole cells (expressed as number of myofibers per mm^2) and manually tracing their minor diameter, whose length was automatically measured by the software. Within each ROI photographed at 10 × magnification, the software semi-automatically calculated, on the basis of the different colors, the area occupied by interstitial tissue and that occupied by myofibers. The amount of connective tissue was calculated as the area occupied by interstitial tissue divided by the total area occupied by both tissues.

The ratio of type I and type II fibers, expressed as percentage of total fibers, and the minor diameter for each fiber type were measured on an equivalent ROI after histochemistry.

Transmission electron microscopy

The samples collected from the remaining six animals were fixed with 2.5% glutaraldehyde in 0.1 M sodium cacodylate buffer (pH 7.2) for 24 h, then postfixed with 1% osmium tetroxide, subsequently dehydrated with acetone and embedded in Durcupan (Fluka Chemie, Buchs, Switzerland). Ultrathin sections (~70 nm) were cut with a diamond blade, stained with 3% uranyl acetate and lead citrate, and observed by a JEOL transmission electron microscope (JEM 2200 FS, Tokyo, Japan) operating at 80 keV.

Statistical analysis

Histomorphometric data for each UM part of the considered subjects were expressed as medians and quartiles. The data were analyzed with Kruskal–Wallis test and *post hoc* Wilcoxon rank sum test. All analyses were performed with PAST statistical software package version 3.0 (http://folk.uio.no/ohammer/past; Hammer & Harper, 2001). Statistical significance was assigned to $P < 0.05$.

Results

Gross morphology

After removal of the osseous pelvic structures, the male pig urethra appears surrounded by connective tissue, without any muscular connection to the pelvic floor. After removal of the connective tissue, the UM appears to surround the pelvic urethra from the bladder neck to the central tendon of perineum (Fig. 1). It has a length of about 16 cm and, in its initial part, is in close relationship with the vesicular glands and prostate, while towards the terminal tract of the pelvic urethra, an extension of the caudal part of the UM embraces the bulbourethral glands (Fig. 1a). Just caudal to the body of the prostate, the whole complex UM shows a marked shrinkage. After removal of vesicular glands, prostate and bulbourethral glands from the dorsal aspect of the pelvic urethra, a longitudinal raphe, extending in the caudal direction from the shrinkage that follows the body of the prostate, is evident. Both longitudinal and transversal sections of the pelvic urethra (Fig. 2a) show the origin of

COLOR

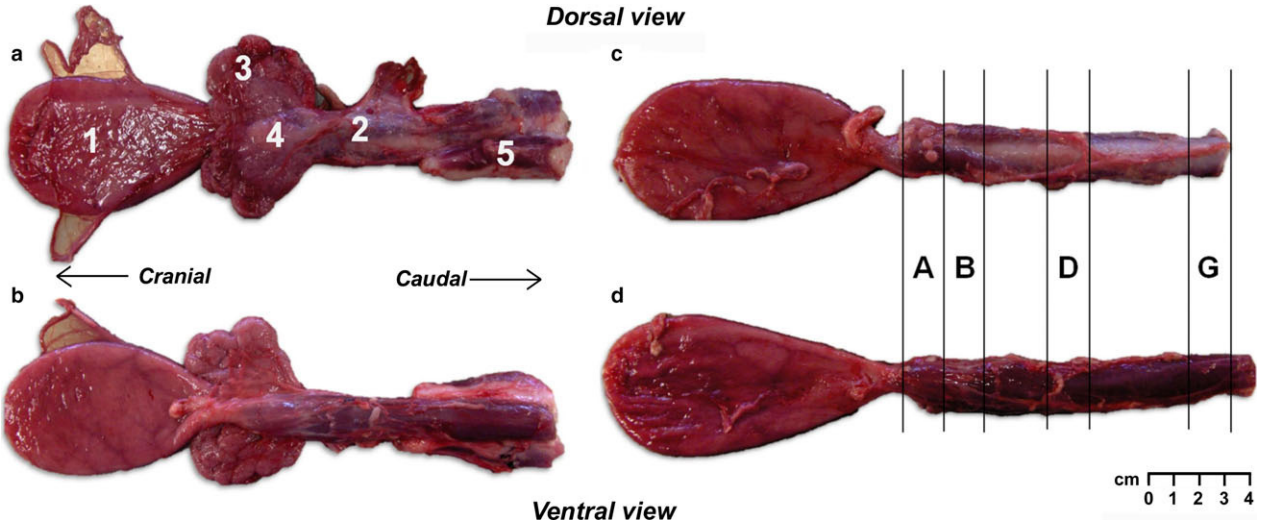

Fig. 1 Macroscopic view of the male pig lower urinary tract. (a) Dorsal view of bladder (1), urethra (2), vesicular glands (3), body of the prostate (4), bulbo-urethral glands (5) after removal of the osseous pelvic structures. (b) Ventral view of the same structures of (a). (c) Dorsal view of the bladder and urethra after removal of the accessory genital glands. (d) Ventral view of the same structures of (c). Lines and capital letters on the right indicate the four parts of the pelvic urethra collected for the study.

the UM with a few longitudinal fibers ventral to the bladder neck. Then the UM expands dorsolaterally to embrace the urethra until it forms a nearly complete 8-mm-thick sphincter just caudal to the body of the prostate. Moving caudally, the UM thickness decreases slightly (5 mm) and the muscle assumes a distinct horseshoe shape, with a dorsal longitudinal raphe. Also the UM fibers that extend to surround the bulbourethral glands still remain separated on the median plane. The cranial tract of the urethral wall is thick and uncompressible due to the presence of the disseminate prostate crossed, near the bladder neck, by the outlets of the vas deferens and the excretory ducts of the vesicular glands and body of the prostate. In correspondence of the post-prostatic shrinkage, the glandular component appears smaller, while the muscular coat is thicker and its two dorso-lateral ends are very close. More caudally and till the caudal end of the pelvic tract, the UM becomes thinner with its two dorsolateral ends that do not cover the entire dorsal surface of the urethra.

An interesting feature, not clearly visible in fresh cross-section of the whole organ, becomes evident in frozen section (Fig. 2c). In the cranial tract of the urethra and, particularly, in the part that labeled B, the UM appears consisting of two juxtaposed layers; the innermost appears dark red, the outermost is thicker and pale. Moving more caudally, the darker inner layer gradually disappears and the UM is composed only by the pale component.

Histological and histomorphometric analysis

In cross-sections of the urethra, the UM appears as a part of a muscular complex composed of an inner layer of smooth muscle and an outer layer of striated muscle that are not separated by fascial planes. The smooth musculature is composed of differently orientated bundles immersed in a conspicuous elastic fibers net. At the level of the internal ostium of urethra, they completely surround the bladder neck with an helical path (Fig. S1), but this organization is soon after modified by the presence of the prostate and, in its further course in the urethra, the smooth muscle contributes to the formation of the glandular fibromuscular stroma (Fig. 2b). The striated muscle, instead, is horseshoe shaped, covering the ventral and lateral sides of the urethra, and is less distinct toward the bladder, but becomes more marked and thick caudally to the body of the prostate (Fig. 2a,b).

Histological observation confirms the bilayer structure of the striated muscle. As it is particularly evident in part B, this part has been further subdivided into 'B int', corresponding to the inner layer of darker musculature visible in frozen section, and 'B ext', corresponding to the outer and paler layer. The internal leaflet, characterized by small fibers, embedded in an abundant connective tissue framework richly vascularized, starts cranially with a few longitudinal fibers (Fig. 2c, A) on the ventral aspect of the urethra.

Moving caudally, the fibers increase their number becoming circumferentially oriented (Fig. 2c, B int). In correspondence of the external paler and thick layer visible in frozen sections myofibers appear larger and compact. More caudally, this structure becomes predominant, while the inner layer becomes thinner and disappears. Its large fibers are longitudinally oriented in cross-sections of the urethra just caudal to the body of the prostate (Fig. 2c, B ext), they assume a more marked circumferential orientation in the

COLOR

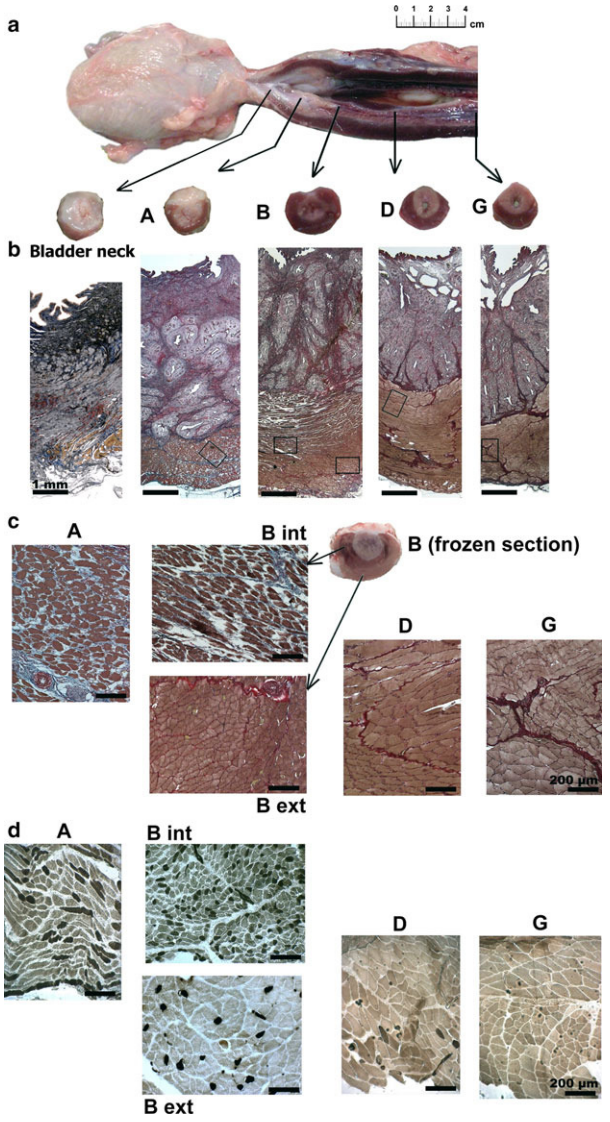

Fig. 2 (a) Longitudinal section along the ventral side of the urethra that allows to evaluate the thickness of the different layers of the wall. Above the longitudinal section, fresh transversal sections of the pelvic urethra show the morphology of the bladder neck and the cranial aspect of each selected part. (b) Photomicrographs showing the structure of the ventral part of the urethral wall in cross-sections corresponding to those of Fig. 1(a), stained with Masson Trichrome and viewed with light microscopy at 1 × magnification. Note the thickness of the disseminate prostate, and the variable aspect and orientation of the UM myofibers. (c) Magnification 10 × of the parts of UM indicated by rectangles in (b). For part B is shown also a peculiarity of its frozen section: the inner layer of the UM appears dark red, and surrounded by a thick and paler layer of musculature. Note the similar aspect of the myofibers (very small and not compact) and of the surrounding connective tissue in part A and B int. The myofibers are wider and compact in B ext, D and G. (d) Photomicrographs of cross-sections of the same parts of UM stained for myofibrillar ATPase with preincubation at pH 4.2. Type I fibers appear dark, type II fibers are light. Magnification 10 ×.

middle part of the pelvic urethra (Fig. 2c, D), then form bundles of variable orientation in correspondence of the bulbourethral glands (Fig. 2c, G).

In all sections, the UM fibers present a wide variation of shape, including round, angulated and polygonal fibers as they were interwoven at various angles to one another. Moreover, at high magnification (> 40 ×), the longitudinal arrangement of myofibrils, and even their striation, is often also evident in the apparent cross-sections of the myofibers (Fig. S2a,b). So, they are not cut perpendicular to their longitudinal axis, as might be expected given the shape of the cell in the section, but it is as if the myofibrils, within the myofibers, had a wavy pattern. Thus, attempts to obtain cross-sections result in a combination of transverse and longitudinal fibers in each direction in which the specimens were cut. The choice to measure, for the morphometric analysis, the minor diameter of the fibers that is, theoretically, the index least affected by the obliquity of fiber sectioning, is precisely due to the impossibility of obtaining sections in which the majority of the fibers were cut transversely.

Notwithstanding the presence of a conspicuous nervous component made up of nerve trunks of various thickness, careful examination of serial sections fails to demonstrate the presence of muscle spindles. Orcein staining allows to recognize as elastic a conspicuous component of the fibers that surrounds the muscular cells (Fig. S2c,d).

The histomorphometric parameters (Fig. 3; Table S1) are significantly different among the various parts of the UM ($P < 0.001$). The number of fibers is significantly higher in part A and B int, where myofibers are smaller and less compact (Fig. 2c, A, B int), as compared with B ext, D and G, where myofibers are larger and more compact (Fig. 2c, B ext, D, G).

Histochemistry

Histochemistry analysis proves that in the pig UM the predominant population is represented by type II fibers, while type I fibers reach at most 30% and are exclusively localized in the cranial tract of the UM. Statistically significant differences among the various parts ($P < 0.001$; Fig. 4; Table S2) seem due to the significant decrease of type I fibers ratio, with contextual increase of that of type II, passing from A to G (Fig. 2d). Regarding the size, in all parts, the diameter of type I fibers resulted significantly smaller as compared with type II.

Electron microscopy

Transmission electron microscopy investigation of the UM confirms the histological analysis, showing fibers and myofibrils in multiple directions (Fig. 5). While in parts A and B, both type I and type II fibers are recognizable, due to proper morphological features, in parts D and G only type II fibers are present. Clusters of large, polymorphic mitochondria and a limited sarcoplasmic reticulum along with broader Z-disks and M-lines typify the type I fibers.

POOR QUALITY FIG

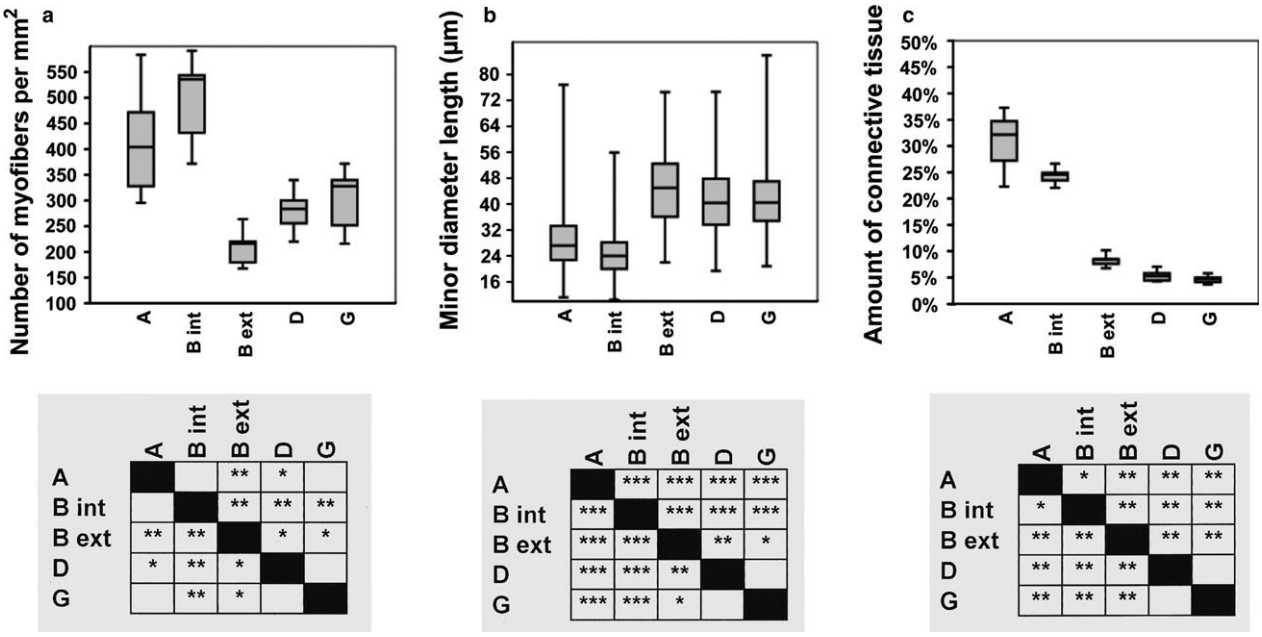

	A	B int	B ext	D	G
A			**	*	
B int			**	**	**
B ext	**	**		*	*
D	*	**	*		
G		**	*		

	A	B int	B ext	D	G
A		***	***	***	***
B int	***		***	***	***
B ext	***	***		**	*
D	***	***	**		
G	***	***	*		

	A	B int	B ext	D	G
A		*	**	**	**
B int	*		**	**	**
B ext	**	**		**	**
D	**	**	**		
G	**	**	**		

Fig. 3 Box plot of the histomorphometric parameters for the different parts of the UM in six animals and their statistical significances: (a) density of myofibers; (b) minor diameter length of the myofibers; (c) amount of connective tissue. Box extension is from the 25th to the 75th percentile, with a line at the median (50th percentile). Asterisks in the tables below the graphs show significant difference $*P < 0.05$; $**P < 0.01$; $***P < 0.001$.

Instead, few mitochondria and a wide sarcoplasmic reticulum along with narrow Z-disks and M-lines typify the type II fibers. Numerous and broad mitochondria are preferentially located in the intermyofibrillar space and closely associated with the sarcoplasmic reticulum. It should be noted that, compared with other skeletal muscles, the mitochondria are less represented in the sub-sarcolemmal space. Glycogen and lipid droplets are also detectable in the intermyofibrillar space.

Discussion

To the best of the authors' knowledge, for the swine species, detailed anatomical studies of the UM were performed previously only in the female (Dass et al. 2001; Zini et al. 2006). A comparison between what was observed in male pigs and what is reported about human UM reveals similarities as well as significant differences. As in humans (Koraitim, 2008), the male pig UM makes part of a cylindrical muscular complex, composed of an inner layer of smooth muscle and an outer layer of striated muscle. The pig UM shape resembles that described for humans before puberty (Oelrich, 1980), when the body of the prostate, which develops from the urethral wall, is small.

In humans, lacking the disseminate prostate, a massive growth of the body of the gland occurs at puberty. This thins and atrophies the overlying muscle, while incorporating other parts within the prostatic perimeter. Structural differences also exist, due to the mechanics of the urinary system, as in humans, besides pressure generated by the bladder wall, urethra also operate gravitational forces that are different in relation to body size, vertical/horizontal stance and lifestyle (e.g. frequency of bladder emptying, house training, rapid flow, or spurts for marking, etc.). Despite this, in both species, the portion of the UM proximal to the bladder forms a short internal leaflet continuing, without distinction, the innermost layer of smooth muscle, and an external layer that is continuous with the muscle surrounding the caudal part of the pelvic urethra. The internal layer of striated muscle, in pig, is composed of very small myofibers surrounded, as in humans (Hinata et al. 2013), by an abundant interstitium composed of collagen with intermingled elastic fibers. In this leaflet, the percentage of slow-twitch (type I) fibers is about 20%. A similar proportion was found in dog (Van der Werf et al. 2000), while in man type I fibers represented the dominant population (Elbadawi, 1996). In pigs, the two layers of striate muscle begin to overlap in correspondence of the body of the prostate, and together form a sort of complete sphincter caudally to the body of the prostate. More caudally, the inner layer thins and disappears. Almost all of the myofibers of the external layer are fast-twitch, more compact and nearly twice as large as those of the inner layer. This external layer might correspond to the 'much bulkier external component' of the UM described in humans (Elbadawi, 1996) and, also in man, the part of UM caudal to the body of the prostate is composed almost exclusively of fast-twitch fibers. The presence of fast-twitch fibers had been categorically

POOR QUALITY FIG

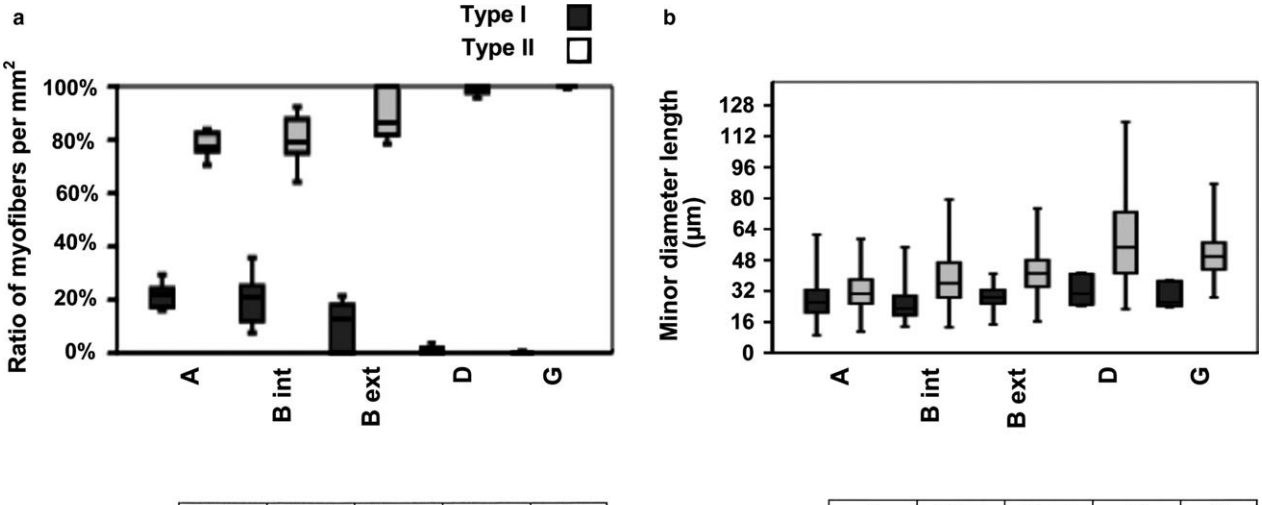

		A		B int		B ext		D		G	
		Type I	Type II	Type I	Type II	Type I	Type II	Type I	Type II	Type I	Type II
A	Type I		**		***	*	**	**	**	*	*
	Type II	**		***		**	*	**	**	*	*
B int	Type I		***		***	*	***	***	***	**	**
	Type II	***		***		***	*	***	***	**	**
B ext	Type I	*	**	*	***		***	*	***	*	**
	Type II	**	*	***	*	***		***	*	**	*
D	Type I	**	**	***	***	*	***		***		**
	Type II	**	**	***	***	***	*	***		**	
G	Type I	*	*	**	**	*	**		**		**
	Type II	*	*	**	**	**	*	**		**	

		A		B int		B ext		D		G	
		Type I	Type II	Type I	Type II	Type I	Type II	Type I	Type II	Type I	Type II
A	Type I		***		***		***		***		***
	Type II	***		***	***		***		***		***
B int	Type I		***		***	*	***	*	***		***
	Type II	***	***	***		**	***		***		***
B ext	Type I			*	**		***		***		***
	Type II	***	***	***	***	***			***	*	***
D	Type I			*					**		**
	Type II	***	***	***	***	***	***	**		**	**
G	Type I						*		**		**
	Type II	***	***	***	***	***	**	**	**	**	

Fig. 4 Box plot of the histomorphometric parameters for the different parts of the UM in six animals and their statistical significances: (a) ratio of the myofibers of type I and type II; (b) minor diameter length of the myofibers. Box extension is from the 25th to the 75th percentile, with a line at the median (50th percentile). Asterisks in the tables below the graphs show significant difference $*P < 0.05$; $**P < 0.01$; $***P < 0.001$.

denied in the human UM in one of the first ultrastructural and histochemical studies (Gosling et al. 1981) performed on biopsies obtained from patients undergoing total cystectomy, therefore, presumably from elderly subjects and on parts of the UM proximal to the bladder. However, later studies unequivocally proved in various species (Elbadawi, 1996) the presence of type II fibers, and in man (Schrøder & Reske-Nielsen, 1983; Tokunaka et al. 1990; Elbadawi et al. 1997; Ho et al. 1998) about one-third of the total fibers resulted fast-contracting. The ratio of the fast- and slow-twitch myofibers varies between species (Creed & Van der Werf, 2001) and individuals, depending on age or body composition (Sumino et al. 2006), and may be significant for the auxiliary role of UM in voiding (Lehtoranta et al. 2006).

The cranial tract of the pig UM contains type I myofibers localized only ventrolaterally and close to the lumen, individually scattered in the dominant population of larger fast-twitch myofibers. This distribution recalls that described in rabbit (Okamura et al. 1989), dog (Van der Werf et al. 2000), (Augsburger & Cruz-Orive, 1994) and calf (Sautet et al. 1987), even though in the latter two species type I fibers were wider and more numerous in the caudal part of the UM. The reason why these fibers, presumably suitable to maintain a slow durable contraction, surround only a rather rigid tract of the urethra and are embedded in an abundant net of collagen and elastic fibers is not clear. According to previous studies (Chen & Creed, 2004; Sumino et al. 2006), the general small size of the fibers of the UM could make the contraction of this muscle faster but weaker and less well maintained than in other skeletal muscles. However, just the shorter diffusion distance for metabolic substrates could ensure a certain fatigue resistance to the myofibers of the UM, compared with those of other skeletal muscles. Moreover, the connective tissue, and in particular the elastic fibers, may help the myofibers in maintaining tone. Also the underlying layer of smooth muscle, which shares some features with the UM, such as variable orientation of the bundles of myofibrils inside of myofibers, the small size of the cells, the fact that the myofibers are bundled by elastic tissue and the lack of muscle spindles, could provide a contribute to the tonic closure of urethra. So it was suggested that these fibers could be implicated in continence. The tract of the UM localized just caudal to the

POOR QUALITY FIG

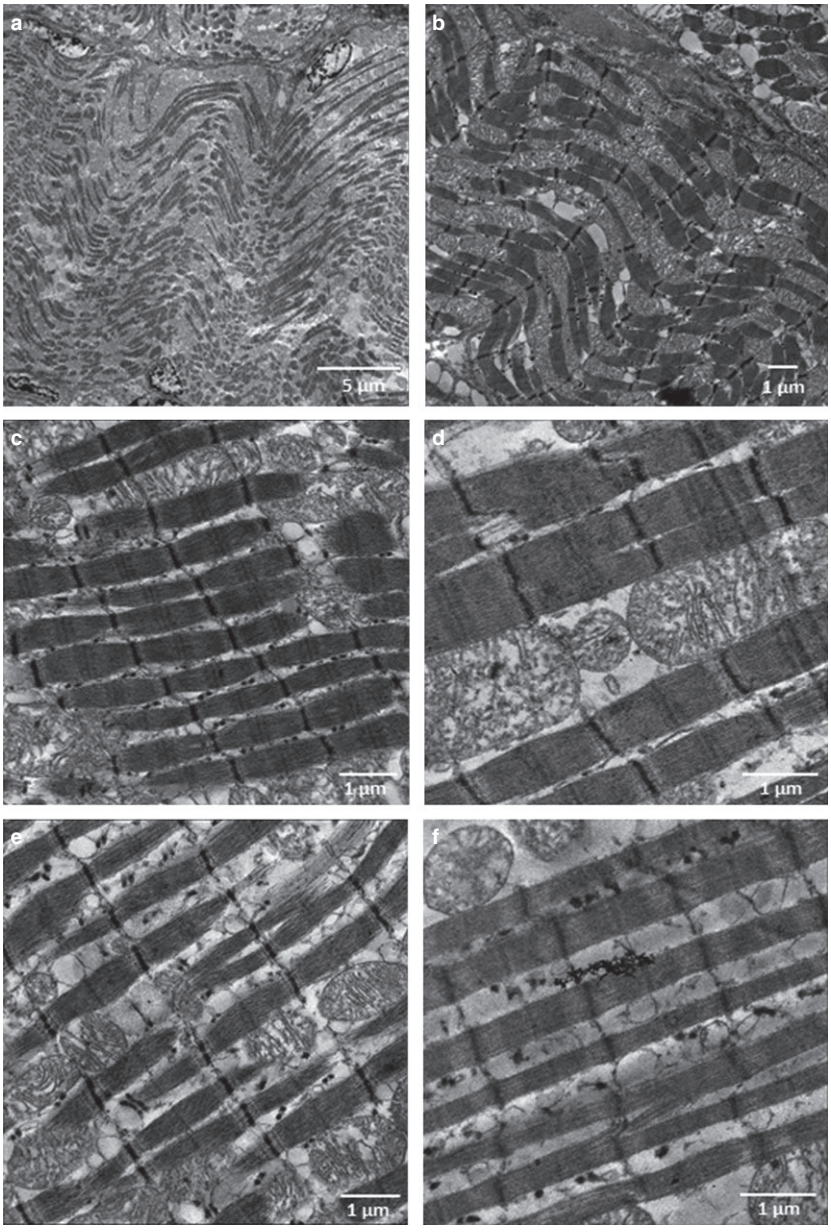

Fig. 5 Transmission electron micrographs of the UM. Myofibrils in multiple directions (a, b); type I fibers characterized by large mitochondria, limited sarcoplasmic reticulum and broader Z-disk (c, d); type II fibers characterized by few mitochondria, wide sarcoplasmic reticulum and narrow Z-disk (e, f). 10

body of the prostate, shaped like an almost complete ring around the urethra and still containing both types of fibers, in addition to voiding, may have a role in blocking the retrograde ejaculation, as postulated for a similar disposition of the fibers of the UM in the rat (Lehtoranta et al. 2006).

According to studies performed on dog (Creed & Van der Werf, 2001), cat (Wang et al. 1999) and rat (Biérinx & Sebille, 2006), the predominance of fast fibers in the caudal part of the UM is consistent with phasic contractions, therefore it is imaginable that the rhythmic activity of the striated sphincter, probably acting as a peristaltic pump, exists during micturition as well as during ejaculation. So also in the pig the caudal tract of the UM may be involved in the voiding mechanism besides in continence.

Conclusion

Both male pig and human UM present structurally and functionally differentiated parts that may be associated to active continence during stress conditions and anterograde semen and urine propulsion. Some differences in the morphology and structure of the UM in the two species seem due to the morphology of the accessory genital glands that develop from the urethral wall and to the different effect of gravity between quadruped and bipedal mammals on the mechanics of the urinary system. So, like for other animals of comparable size, such as large dogs and sheep, the results of eventual studies on the continence mechanism cannot be transferred without reservation from pigs to humans.

However, the male pig UM is well developed, and hence might be well suited for physiological studies on isolated muscle strips. Moreover, the swine species has been used as an animal model for the preclinical evaluation of novel cell-based therapies aimed to strengthen the UM (Mitterberger et al. 2007; Herrera-Imbroda et al. 2015) as treatment for male stress urinary incontinence following iatrogenic sphincter damage. So, the detailed description of the swine UM given with the present study could be useful in studies aimed to control and document functional and histological changes following the autologous injection of myoblasts or stem cells into the porcine urethra, practice that is still controversial, as the cells can initiate inflammatory reactions. Therefore, beside guinea-pig (Will et al. 2015), also the swine species could be used as an animal model to get a detailed overview of the cell behavior *in vivo*.

Acknowledgements

Research by the authors was made thank to the Research Project Grant FIL 2009 – University of Parma.

Conflict of interest

The authors declare that they have no conflict of interest.

References

Augsburger HR, Cruz-Orive LM (1994) Morphological, histochemical and stereological analysis of the female canine M. urethralis. *Histochemistry* **102**, 373–382.

Biérinx AS, Sebille A (2006) The urethral striated sphincter in adult male rat. *Anat Embryol (Berl)* **211**, 435–441.

Borirakchanyavat S, Baskin LS, Kogan BA, et al. (1997) Smooth and striated muscle development in the intrinsic urethral sphincter. *J Urol* **158**, 1119–1122.

Brooke MH, Kaiser KK (1970) Three "myosin adenosine triphosphatase" systems: the nature of their pH lability and sulfhydryl dependence. *J Histochem Cytochem* **18**, 670–672.

Chen X, Creed KE (2004) Histochemical and contractile properties of striated muscles of urethra and levator ani of dogs and sheep. *Neurourol Urodyn* **23**, 702–708.

Creed KE, Van der Werf BA (2001) The innervation and properties of the urethral striated muscle. *Scand J Urol Nephrol Suppl* **???**, 8–11; discussion 106–125.

Dass N, McMurray G, Greenland JE, et al. (2001) Morphological aspects of the female pig bladder neck and urethra: quantitative analysis using computer assisted 3-dimensional reconstructions. *J Urol* **165**, 1294–1299.

Elbadawi A (1985) Ultrastructure of vesicourethral innervation. III. Axoaxonal synapses between postganglionic cholinergic axons and probably SIF-cell derived processes in the feline lissosphincter. *J Urol* **133**, 524–528.

Elbadawi A (1996) Functional anatomy of the organs of micturition. *Urol Clin North Am* **23**, 177–210.

Elbadawi A, Mathews R, Light JK, et al. (1997) Immunohistochemical and ultrastructural study of rhabdosphincter component of the prostatic capsule. *J Urol* **158**, 1819–1828.

Gosling JA, Dixon JS, Critchley HO, et al. (1981) A comparative study of the human external sphincter and periurethral levator ani muscles. *Br J Urol* **53**, 35–41.

Hammer Ø, Harper DAT (2001) Past: paleontological statistic software package for education and data analysis. *Paleontol Electron* **???**, 1–9.

Herrera-Imbroda B, Lara MF, Izeta A, et al. (2015) Stress urinary incontinence animal models as a tool to study cell-based regenerative therapies targeting the urethral sphincter. *Adv Drug Deliv Rev* **82–83**, 106–116.

Hinata N, Murakami G, Abe S, et al. (2013) Coexistence of elastic fibers with hyaluronic acid in the human urethral sphincter complex: a histological study. *J Urol* **190**, 1313–1319.

Ho KM, McMurray G, Brading AF, et al. (1998) Nitric oxide synthase in the heterogeneous population of intramural striated muscle fibres of the human membranous urethral sphincter. *J Urol* **159**, 1091–1096.

Koraitim MM (2008) The male urethral sphincter complex revisited: an anatomical concept and its physiological correlate. *J Urol* **179**, 1683–1689.

Lehtoranta M, Streng T, Yatkin E, et al. (2006) Division of the male rat rhabdosphincter into structurally and functionally differentiated parts. *Anat Rec A Discov Mol Cell Evol Biol* **288**, 536–542.

Mitterberger M, Pinggera GM, Marksteiner R, et al. (2007) Functional and histological changes after myoblast injections in the porcine rhabdosphincter. *Eur Urol* **52**, 1736–1743.

Neuhaus J, Dorschner W, Mondry J, et al. (2001) Comparative anatomy of the male guinea-pig and human lower urinary tract: histomorphology and three-dimensional reconstruction. *Anat Histol Embryol* **30**, 185–192.

Oelrich TM (1980) The urethral sphincter muscle in the male. *Am J Anat* **158**, 229–246.

Okamura K, Tokunaka S, Fujii H, et al. (1989) Histochemical study of external urethral sphincter in the rabbit. Analysis with construction of histograms. *Nihon Hinyokika Gakkai Zasshi* **80**, 1127–1133.

Sautet JY, Amara A, Cabanie P, et al. (1987) The urethral muscle (musculus urethralis) of the female calf. Anatomical, histological, histochemical and morphometrical data. *Acta Anat (Basel)* **130**, 366–372.

Schrøder HD, Reske-Nielsen E (1983) Fiber types in the striated urethral and anal sphincters. *Acta Neuropathol* **60**, 278–282.

Stolzenburg JU, Schwalenberg T, Do M, et al. (2002) Is the male dog comparable to human? A histological study of the muscle systems of the lower urinary tract. *Anat Histol Embryol* **31**, 198–205.

Strasser H, Ninkovic M, Hess M, et al. (2000) Anatomic and functional studies of the male and female urethral sphincter. *World J Urol* **18**, 324–329.

Sumino Y, Sato F, Kumamoto T, et al. (2006) Striated muscle fiber compositions of human male urethral rhabdosphincter and levator ani. *J Urol* **175**, 1417–1421.

Tokunaka S, Murakami U, Okamura K, et al. (1986) The fiber type of the rabbits' striated external urethral sphincter: electrophoretic analysis of myosin. *J Urol* **135**, 427–430.

Tokunaka S, Okamura K, Fujii H, et al. (1990) The proportions of fiber types in human external urethral sphincter: electrophoretic analysis of myosin. *Urol Res* **18**, 341–344.

Van der Werf BA, Hidaka T, Creed KE (2000) Continence and some properties of the urethral striated muscle of male greyhounds. *BJU Int* **85**, 341–349.

Wang B, Bhadra N, Grill WM (1999) Functional anatomy of the male feline urethra: morphological and physiological correlations. *J Urol* **161**, 654–659.

Whitmore I, Gosling JA, Gilpin SA (1984) A comparison between the physiological and histochemical characterisation of urethral striated muscle in the guinea pig. *Pflugers Arch* **400**, 40–43.

Will S, Martirosian P, Eibofner F, et al. (2015) Viability and MR detectability of iron labeled mesenchymal stem cells used for endoscopic injection into the porcine urethral sphincter. *NMR Biomed* **28**, 1049–1058.

Zini L, Lecoeur C, Swieb S, et al. (2006) The striated urethral sphincter of the pig shows morphological and functional characteristics essential for the evaluation of treatments for sphincter insufficiency. *J Urol* **176**, 2729–2735.

Supporting Information

Additional Supporting Information may be found in the online version of this article:

Fig. S1. (a) Photomicrograph showing an histological cross-section of the male pig bladder neck at the level of the internal ostium of urethra (Masson trichrome staining, magnification 1 ×). The muscle layer (*) is composed exclusively of smooth muscle bundles frequently changing their orientation and recalling an helical path. They are in continuity with the ones of the M. detrusor vesicae (#). (b) Macroscopic ventral view of the male pig lower urinary tract. The arrow indicates the level of the cross-section of (a).

Fig. S2. Photomicrographs showing particular aspects of apparent transversal and longitudinal sections of the myofibers of male pig UM at high magnification. (a) Cell shape would suggest that they were sectioned transversely, but the arrangement of myofibrils within them is variable. In some areas of the cells myofibrils appear as dots, and were therefore sectioned transversely, in other areas of the same cells myofibrils appear arranged lengthwise. (b) In longitudinal section, the myofibrils within the myofibers show a wavy pattern. (Masson trichrome staining, magnification 60 ×.) (c) Photomicrograph of a section of UM in part B int. and (d) in part G. Black arrows indicate elastic fibers surrounding muscular cells (Orcein staining, magnification 40 ×).

Table S1. Histomorphometric data obtained in different parts of the UM of six male pigs.

Table S2. Histomorphometric data of type I and type II myofibers in different parts of the UM of six male pigs.

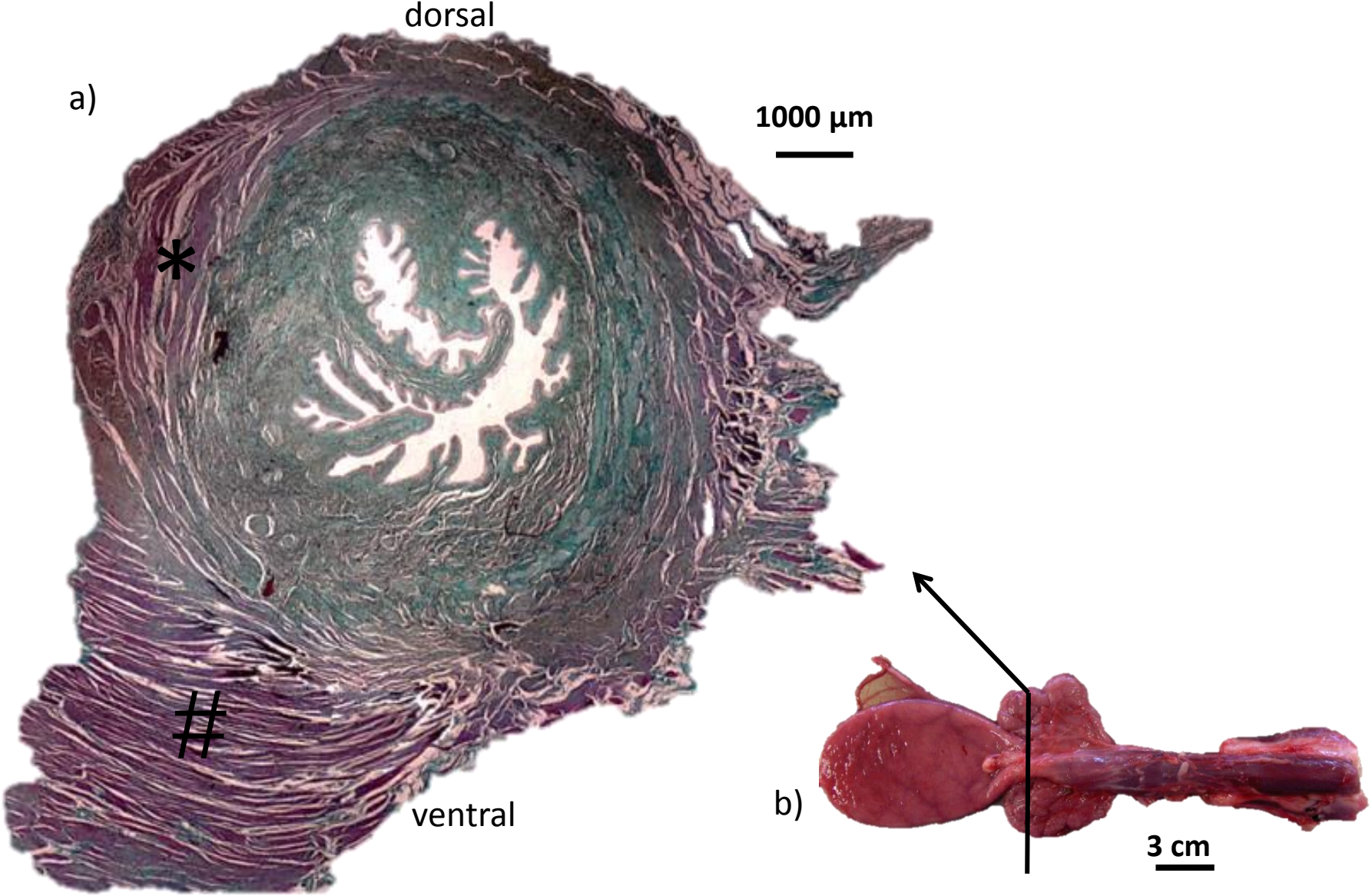

Supplementary Figure S1 a) Photomicrograph showing an histological cross section of the male pig bladder neck at the level of the internal ostium of urethra (Masson trichrome staining, Magnification 1X). The muscle layer (*) is composed exclusively of smooth muscle bundles frequently changing their orientation and recalling an helical path. They are in continuity with the ones of the *M. detrusor vesicae (#).* b) Macroscopic ventral view of the male pig lower urinary tract. The arrow indicates the level of the cross section of figure S1a)

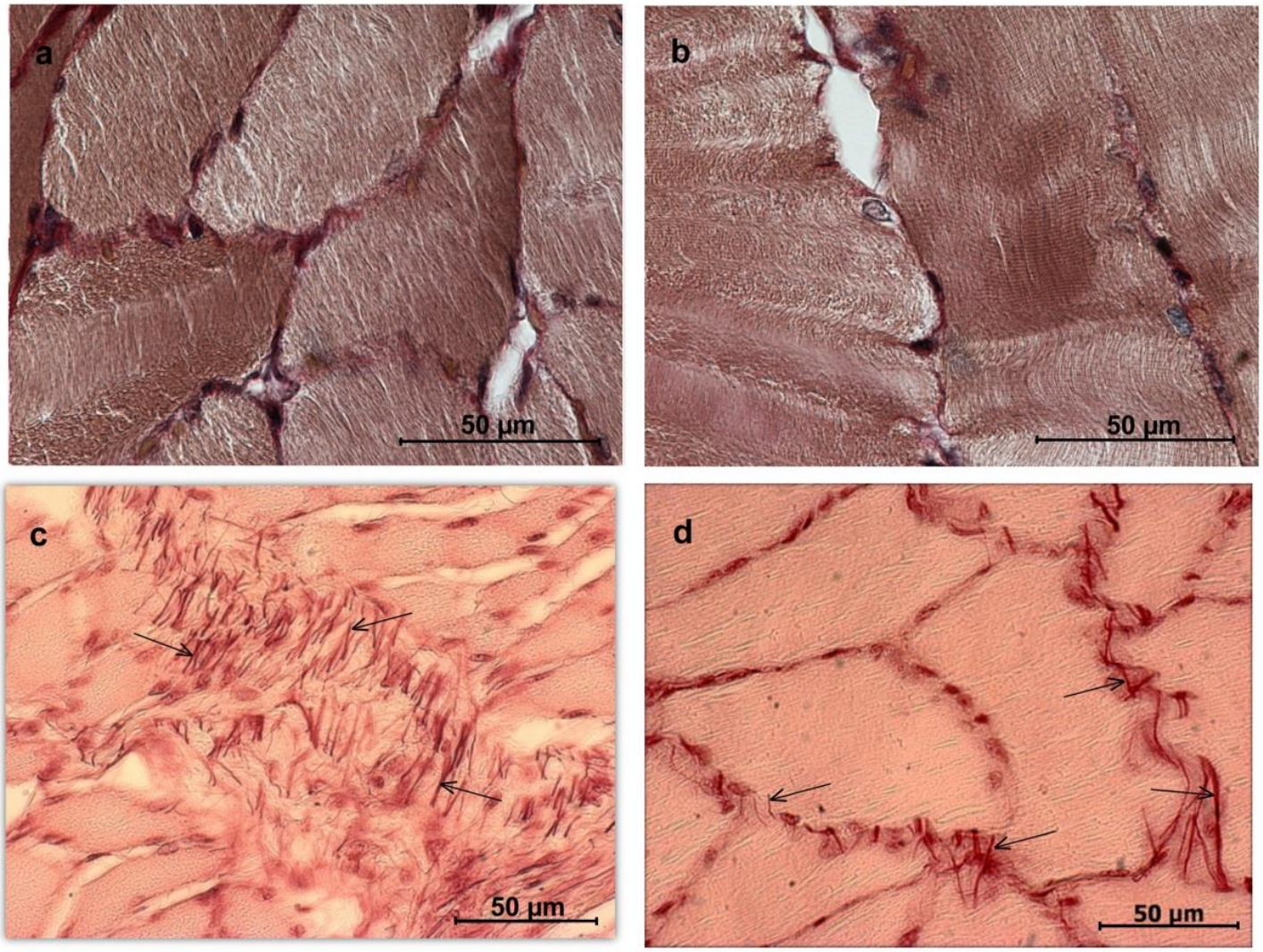

Supplementary Figure S2 Photomicrographs showing particular aspects of apparent transversal and longitudinal sections of the myofibers of male pig urethral muscle at high magnification. a) Cell shape would suggest that they were sectioned transversely, but the arrangement of myofibrils within them is variable. In some areas of the cells myofibrils appear as dots, and were therefore sectioned transversely, in other areas of the same cells myofibrils appear arranged lengthwise. b) In longitudinal section, the myofibrils within the myofibers show a wavy pattern. (Masson trichrome staining, Magnification 60X) c) Photomicrograph of a section of urethral muscle in part B int. and d) in part G. Black arrows indicate elastic fibers surrounding muscular cells (Orcein staining, Magnification 40X)

SUPPLEMENTARY TABLE S1. ***Histomorphometric data obtained in different parts of the urethral muscle (UM) of 6 male pigs***

part of the UM	Medians (25th and 75th percentiles in brackets)		
	number of myofibers/mm^2	minor diameter length (µm)	amount of connective tissue
A	392 (320 500)	27.2 (22.8 33.3)	31.4% (26% 35.4%)
B int	518 (417 556)	24.1 (20 28.2)	24.5% (23.2% 25.4%)
B ext	210 (177 231)	45.2 (36.3 52.4)	8.5% (7.4% 8.9%)
D	274 (247 310)	40.7 (33.8 47.9)	5% (4.4% 6.2%)
G	320 (243 348)	40.5 (34.8 47)	4.7% (4.1% 5.2%)

SUPPLEMENTARY TABLE S2. ***Histomorphometric data of type I and type II myofibers in different parts of the urethral muscle (UM) of 6 male pigs.***

part of the UM	type of myofibers	Medians (25th and 75th percentiles in brackets)		
		number of myofibers / mm^2	ratio of myofibers / μm^2	minor diameter length (μm)
A	type I	100 (54 100)	22.6% (17.4% 24.2%)	26.2 (21 32.7)
	type II	425 (155 475)	77.4% (75.8% 82.6%)	30.5 (25.5 38)
B int	type I	100 (75 150)	20.7% (12.1% 25%)	23.3 (19.5 29.3)
	type II	400 (325 575)	79.3% (75% 87.9%)	36 (28.7 46.7)
B ext	type I	28 (0 50)	13.3% (0% 18.2%)	28.7 (24.9 32.7)
	type II	275 (225 400)	81.8% (86.7% 100%)	41.1 (34.3 47.9)
D	type I	2 (0 4)	1.5% (0% 2.3%)	32.4 (26.6 39)
	type II	97 (76 247)	98.5% (97.7% 100%)	54.6 (41.3 72.8)
G	type I	0 (0 1)	0% (0% 0.4%)	26.3 (24.6 37.2)
	type II	196 (158 219)	100% (99.6% 100%)	49.9 (43.2 57)